WELDING RESEARCH

SUPPLEMENT TO THE *WELDING JOURNAL,* OCTOBER 2003
Sponsored by the American Welding Society and the Welding Research Council

Theoretical Analysis of Welding Characteristics during Resistance Mash Seam Welding of Sheet Steels

Surface strains and approximate thermal cycles can be easily calculated for resistance mash seam welding and used to infer joint quality

BY J. E. GOULD

ABSTRACT. In this work, the mash seam welding (RSEW-MS) process has been analyzed with respect to the requirements of the different mechanisms of solid-state welding, and the role of each assessed. The process was first analyzed to predict local strains along the weld interface. This was done through a simple geometric analysis of the weld stackup. Thermal cycles were then analyzed using a variation of the 2-D Rosenthal equation and an appropriate heat-generation term for mash seam welding. From this relationship, an equation was deduced defining the duration of temperature excursions above critical temperatures for metallurgical reactions. Calculations of weld interface strains suggest that for mash seam welding, maximum strain levels are on the order of 110%. Further, for realistic lap conditions, the degree of strain appeared to be a function of the setdown of the joint stackup only and not the included lap. In addition, these strains were found to be relatively low compared to published strain requirements for cold pressure welding (400–500%). As a result, it was concluded that actual surface straining plays a reduced role in joining during mash seam welding of sheet steels. In the absence of sufficient strain, solid-state welding must occur by thermally assisted processes. For such processes, longer times at temperature promote such mechanisms as oxide dissolution, diffusion, and weld area recovery/recrystallization. Analysis of thermal excursions above critical metallurgical temperatures suggests that higher currents, slower travel speeds, and increased laps all should improve weld performance. These observations are all consistent with extensive manufacturing experience.

J. E. GOULD is Chief Engineer, Resistance and Solid-State Welding, at Edison Welding Institute, Columbus, Ohio.

Introduction

Resistance mash seam welding is a variant of both conventional resistance seam welding (RSEW) and projection welding (PW). Mash seam welding uses equipment quite similar to that for conventional seam welding, including a large resistance welding frame, and rotating wheel-type electrodes to conduct the current. Mash seam welding differs from conventional seam welding in that the degree of overlap (between the sheets) is relatively small (on the order of 1–2 times the sheet thickness). During welding, this lap area is resistance heated and forged down to form a joint. A schematic representation of the lap prior to welding and the final joint geometry is provided in Fig. 1. This heating and forging characteristic is similar to solid projection welding.

Mash welding is essentially a heating and forging process. Resulting joints are typically of solid-state character, and, when properly formed, show no evidence of melting. Earlier work on mash seam welding (Ref. 1) has suggested that formation of a fusion zone was characteristic of these joints, and this is certainly possible if sufficiently high currents and low travel speeds are used. However, most mash seam welds today are made as solid-state joints. Mash seam welding shows considerable advantage over conventional seam welding in a number of areas. Since a relatively narrow lap is used, this process is quite insensitive to the particular wheel geometry. As a result, the process is usually conducted with relatively wide, flat wheels. These flat wheels offer excellent final surface finish and, in addition, greatly reduce sensitivity of the process to joint tracking. The final joint thickness is also generally very close to the base material thickness (typically 110–130% of that thickness). In addition, with secondary mechanical planishing, final joint thicknesses equal to the base material thickness can be obtained.

Given these advantages, it is not surprising that mash seam welding is widely used in industry today. Applications for mash seam welding include appliance manufacturing (e.g., dryer drums, motor shells) and fabrication of can and drum assemblies, bicycle rims, etc. More recently, mash seam welding has been used in automotive applications for the production of tailor-welded blanks (Refs. 2–4).

It is somewhat surprising that, given the widespread application of this process, the underlying mechanics of joint formation are not well understood. As mentioned above, some work was done to define the characteristics of these joints using metallographic inspection (Ref. 1). However, that work focused on the fusion characteristics of this process, and, as described, most of these joints are now made in the solid-state regime. As a result, this work is not applicable to most mash seam welding applications.

KEY WORDS

Resistance Mash Seam Welding
Solid-State Welding
Strain Analysis
Thermal Cycle Analysis

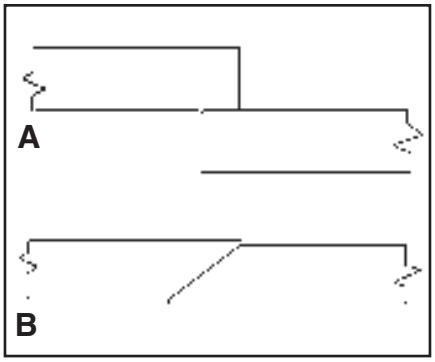

Fig. 1 — Mash seam weld geometry prior and following application of the joining process. A — Before welding; B — after welding.

Recent work has been done to better define the mechanisms of joining during solid-state welding processes (Ref. 5). Welding in these processes appears to occur in three distinct submechanisms. These include the following:

1) Creation of additional surface (surface strains).
2) Dissolution of weld interface contaminants.
3) Dissolution of residual weld interface structure.

Each of these mechanisms can be sufficient to create a joint. For example, simply creating surface strains is the operating mechanism for cold pressure welding (CW), while dissolution of contaminants and residual weld interface structure are the operating mechanisms for diffusion welding (DFW).

These mechanisms of joining appear to be applicable to mash seam welding. Mash seam welding certainly creates additional surface by forging of the joint stackup (configuration of the sheets in the lap area). In addition, the heating done to promote forging can also be used to facilitate dissolution of weld interface contaminants and residual weld interface structures.

In this work, the formation of joints in resistance mash seam welds has been investigated using analytical techniques. This work has included examinations of both the development of surface strains and temperature profiles in these components. The two are then compared and used to define operative mechanisms for creating mash seam welds between sheet steels.

Analysis of the Resistance Mash Seam Welding System

As briefly outlined above, mash seam welding is a combination of two processes: resistance heating and mechanical forging. With respect to the basic mechanisms of welding for solid-state processes, these factors operate somewhat independently.

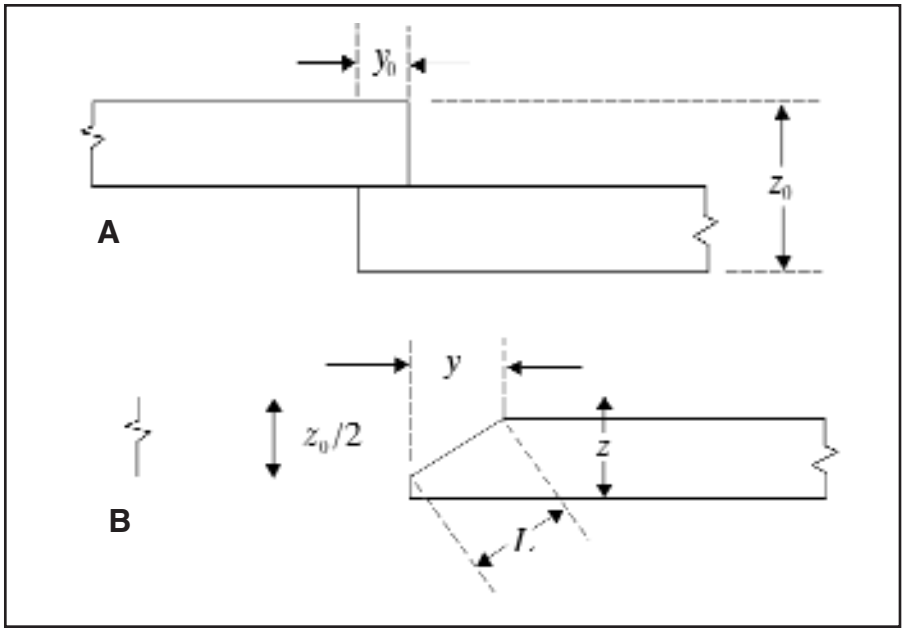

Fig. 2 — Geometry configuration for strain analysis during mash seam welding. A — Before welding; B — during welding.

That is, mechanical forging largely results in the creation of surface strain, while resistance heating provides the thermal energy for dissolution of residual weld interface contaminants and annealing recrystallization of the residual weld interface structure. To gain an understanding of their influence on the process, each aspect can be analyzed separately. This is done in separate sections below.

Analysis of Forging Effects

The role of the application of force is largely to create additional surface along the weld interface. This effect has been well documented, particularly in the area of cold pressure welding (Refs. 6–9). Generally, in mash seam welding, forging is described in terms of the final joint thickness relative to the thickness of the attached sheets. Obviously, for similar thickness sheets, this value can range from 2 prior to welding, down to 1 for a fully collapsed joint. For actual mash seam welds, values for the final joint thickness range from 1.1 to 1.3 times the sheet thickness.

Figure 1 details the shape of the weld interface before and after mash welding. The actual surface strains that occur along the weld interface can be easily derived from the final joint thickness using some simple geometric relationships. This analysis can be conducted based on the following assumptions:

1) During forging, the joint remains geometrically symmetrical about its centerline in cross section.
2) Relative to the joint centerline, material is conserved.
3) The length of the contact area can be defined as a straight line between the termination points of the relative sheets in cross section.

The resulting configuration for analysis is presented in Fig. 2. This figure presents the schematic condition at the beginning and at some point during the forging process. The parameters z_0 and y_0 are defined as twice the sheet thickness and the lap width, respectively. z and y are the actual stackup thickness and apparent lap at any point in the forging process. The above assumptions can be translated into the following equations:

$$y_0 z_0 = yz \tag{1}$$

$$y^2 + \left(\frac{z_0}{2} - z - \frac{z_0}{2}\right)^2 = L^2 \tag{2}$$

In the latter equation, L represents the apparent length of the weld at any point in the forging process. The former equation represents conservation of material. The latter equation simply represents the length of the weld interface as a function of the geometric parameters and can be simplified to

$$y^2 + \left(z_0 - z\right)^2 = L^2 \tag{3}$$

Equations 1 and 3 can then be combined to eliminate the y term and yield the following expression:

$$\frac{y_0^2 z_0^2}{z^2} + \left(z_0 - z\right)^2 = L^2 \tag{4}$$

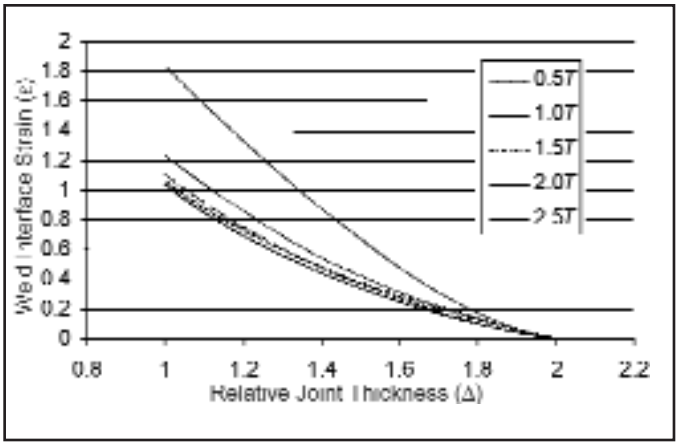

Fig. 3 — Computed values of surface strains (ε) during mash seam welding as a function of the relative lap (ξ) and the relative joint thickness (Δ).

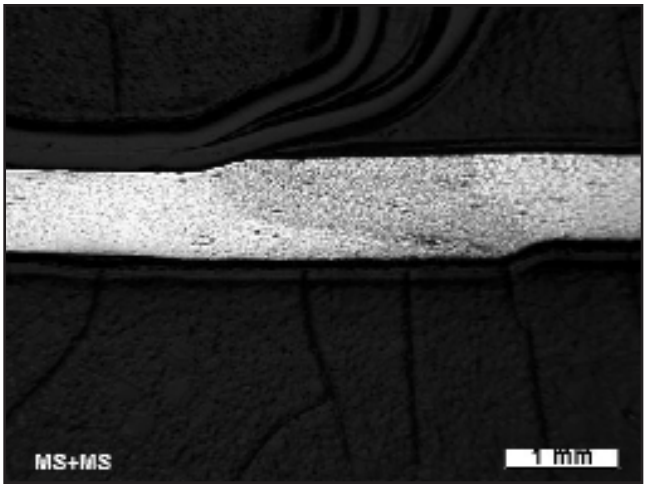

Fig. 4 — A representative mash weld with initial relative lap (ξ) of 1.4, and final relative joint thickness (Δ) of 1.16. (Joint shows a welding strain of 90% compared to a predicted value of 84%.)

Dividing through by y_0^2, and then using the observation that $y_0 = L_0$ (the initial weld interface/lap length) in the right-hand side of the equation, the relationship can be reduced to

$$\left(\frac{z_0}{z}\right)^2 + \frac{1}{y_0^2}(z_0 - z)^2 = \left(\frac{L}{L_0}\right)^2 \qquad (5)$$

Inverting the first term, and then factoring a z_0 out of the second term allows the equation to be reexpressed in the form

$$\frac{1}{\left(\frac{z}{z_0}\right)^2} + \left(\frac{z_0}{y_0}\right)^2\left(1 - \frac{z}{z_0}\right)^2 = \left(\frac{L}{L_0}\right)^2 \qquad (6)$$

Then, the right hand of the expression can be rewritten, and the equation redefined as

$$\frac{1}{\left(\frac{z}{z_0}\right)^2} + \left(\frac{z_0}{y_0}\right)^2\left(1 - \frac{z}{z_0}\right)^2 = \left(\frac{L - L_0}{L_0} + 1\right)^2 \qquad (7)$$

where $(L - L_0)/L_0$ is the effective weld interface strain. Defining the relative joint thickness as $\Delta = 2z/z_0$ (the joint thickness divided by the sheet thickness), the relative lap as $\xi = 2y_0/z_0$ (the lap divided by the sheet thickness), and the weld interface strain as $\varepsilon = (L - L_0)/L_0$, Equation 7 can be rewritten as

$$\left(\frac{2}{\Delta}\right)^2 + \left(\frac{2}{\xi}\right)^2\left(1 - \frac{\Delta}{2}\right)^2 = (\varepsilon + 1)^2 \qquad (8)$$

Thermal Analysis

As described above, heat generation during mash seam welding is largely through resistance heating the lap area itself. As is well known, the rate of heat generation ($\dot{Q}$) for resistance welding processes is generally defined as $\dot{Q} = I^2 R$, where I is the applied welding current and R is the resistance of the workpiece and contact surfaces. For a simple examination of heat generation during mash seam welding, the resistance can be approximated through the conducting volume of the workpiece. This can be defined as $R = \rho z_0/A$, where ρ is the resistivity of the steel and A is the area of contact. This assessment of resistance assumes, of course, no contact resistances, and that the height of the stackup is roughly equal to two times the sheet thickness. These are simplifications but are useful for understanding heat generation during this process. Assuming further that the contact area is bounded by the lap (y_0) and the length of contact (l), the rate of heat generation can be expressed as follows:

$$\dot{Q} = \rho\left(\frac{I}{A}\right)^2 l\, y_0 z_0 \qquad (9)$$

In this equation, the current has been normalized to the contact area.

Once an expression for heat generation has been described, it is a relatively simple process to define the heat-flow equation for this process. Mash seam welding is typically done with thin sheets, and 2-D heat flow predominates. (The wheels themselves typically move at high speeds, minimizing their influence as a heat sink.) As a result, the Rosenthal 2-D solution (Ref. 10) can be used in combination with the heat-generation term defined in Equation 9 above. The resulting expression is as follows:

$$T - T_0 = \left(\frac{I}{A}\right)^2 \frac{\rho l\, y_0}{2\pi K} \exp\left(\frac{-v w}{2\alpha}\right) K_0\left(\frac{v R}{2\alpha}\right) \qquad (10)$$

where $T - T_0$ is the rise from the base temperature, K and α are the thermal conductivity and diffusivity, respectively, v is the welding speed, w and R are distances along and radially away from the heat source, and K_0 is the modified Bessel function of the second kind of zeroth order. Following the work of Adams (Ref. 11) the cooling rates in such a weld can then be expressed as follows:

$$\frac{dT}{dt} = -\frac{2\pi K^2}{\alpha}\left(\frac{v}{\rho\left(\frac{I}{A}\right)^2 l\, y_0}\right)(T - T_0)^3 \qquad (11)$$

Discussion

Effects of Surface Strains

As previously described, the first mechanism of joining during any forge welding process is the creation of additional contact surface. The creation of this additional contact surface essentially fractures weld interface contaminants and allows contact of nascent surfaces, enabling solid-state welding (Ref. 5). The degree of this surface extension is usually described by the surface strain.

For mash seam welding, the amount of surface strain as a function of process con-

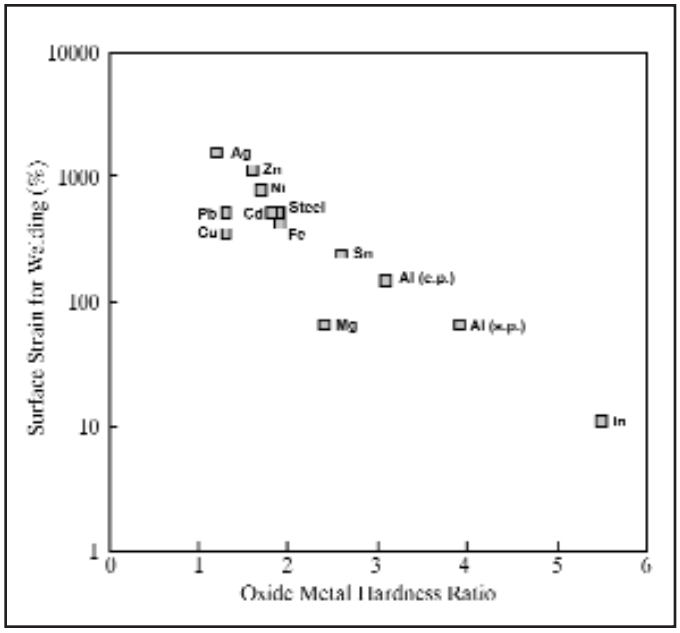

Fig. 5 — Plot showing the relationship between the oxide/metal hardness ratio and the minimum strain for cold welding for different materials.

ditions is defined in Equation 8 above. It is clear from this equation that the amount of surface strain is a function of only the relative initial relative lap (ξ) and the relative joint thickness (Δ). Typically, for real manufacturing applications, the relative lap (ξ) can vary from about 0.5 to 2.5. Further, given geometrical constraints of the process, the relative joint thickness has a value of 2 before any setdown (collapse of the initial joint stackup), with a minimum value of 1 as the joint thickness achieves the base material thickness. Plots showing variations in weld interface strains within these constraints are provided in Fig. 3. Surface strain (ε) is plotted as a function of relative joint thickness (Δ) for five levels of relative lap (ξ).

The extent of weld interface strain is clearly affected by the relative joint thickness. The degree of strain is obviously zero when the joint thickness is twice the sheet thickness (no setdown), and it increases continuously as the relative joint thickness decreases. Maximum strains corresponding to complete setdown (Δ = 1) appear to range from 100 to 180% with relative laps ranging from 0.5 to 2.5.

The effect of relative lap is of greater interest. These results suggest that for relatively small laps (ξ < 1) weld interface strains are very sensitive to lap. However for larger laps (ξ > 1), the relationship is reduced. This suggests, of course, that the highest strains can be obtained with the smallest overlaps.

As mentioned above, typical mash seam welding is done with relative laps on the order of 1–2, and relative final joint thicknesses on the order of 110–130%. In referring to Fig. 3, this range of laps and final joint thicknesses correspond to weld interface strains ranging from about 55–110%.

A representative mash seam weld for tailored-welded blank application is presented in Fig. 4. The weld was made on 0.8-mm-thick mild steel sheets. The initial relative lap (ξ) before welding is 1.4, and final relative joint thickness (Δ) after welding is 1.16. The weld interface strain (ε) measured from this figure is roughly 90%. This is consistent with the calculated value from Equation 8 (84%).

To understand the role surface strains that occur during collapse has on the welding process, the strains calculated here can be compared to those necessary for joining during cold pressure welding. The classical works on cold pressure welding published by Tylecote and his coworkers (Refs. 6, 7) contain information on required fractional deformations for welding for various materials. These measurements were made on lap specimens using an elongated punch. Assuming plane strain conditions under the punch and constancy of volume over the deformed material, an analysis similar to the one described above can be used to relate surface strains to the measured welding deformations. The resulting relationship is as follows:

$$\varepsilon = \frac{\%Def}{100 - \%Def} \qquad (12)$$

where *%Def* is the measured deformations for welding in Tylecote's original work. Critical surface deformations for welding (in the absence of heat) can now be translated from Tylecote's work and are reported in Table 1 below. As has been detailed in numerous works (Refs. 6–9), critical strains for welding are related to the relative hardness of surface oxides. These correlations were made in Tylecote's original work and have been translated and presented as necessary surface strains for welding as a function of this oxide/metal hardness ratio for different materials. These results are presented graphically in Fig. 5.

These results suggest that critical surface strains for welding range from as little as 10% for materials with very brittle oxides, to more than 1000% where the oxides are more ductile. These results further suggest that critical surface strains for steel are in the range of 400–500%. Clearly, these levels are outside the range of possible strains for conventional mash seam welding methods. It appears then, that the forging occurring during mash seam welding of steels plays a reduced role in the overall welding process. These observations are consistent with two commonly observed facts in manufacturing experience. The first is that increases in lap (which apparently do not increase surface strain) are advantageous to weld quality. The second is that metal collapse in the absence of heat does not produce any apparent welding.

Effects of the Thermal Cycle

The above discussion strongly suggests that the first stage of the solid-state welding process, creation of additional surface, plays a reduced role in mash welding steels. As has been discussed elsewhere (Ref. 5), further joining during solid-state welding processes must occur by the addition of thermal energy. As mentioned above, this thermal energy has two functions. Initially, thermally activated dissolution of retained surface oxides occurs, creating additional clean surface for welding. Also, this energy allows recovery (and in the extreme recrystallization) of the residual deformed weld interface structure. For mash welding of steels, the role of this thermal energy appears to predominate.

The thermal response of mash seam welds has been summarized in Equations 10 and 11 above. For resistance welding processes, heating is generally extremely rapid (Ref. 12). Assuming this rapid heating, the time above a specific temperature for metallurgical reaction can be estimated by integrating the cooling rate expression given in Equation 11 above. The resulting equation is as follows:

$$\Delta t = \frac{\alpha}{2\pi} \frac{\left(\rho \left(\frac{I}{A}\right)^2 l y_0\right)^2}{v K} \frac{\Delta T}{T_p^3} \qquad (13)$$

where Δt is the time above critical temperature $T_p - \Delta T$; T_p is the peak or forging temperature (generally 1200–1300°C for mash seam welding); and ΔT is the difference between the peak and critical temperatures. This equation allows the effects

of all critical process parameters on time above critical temperature to be assessed.

It is no surprise that the dominant process variable is the specific welding current (I/A). Times above critical temperatures increase to the fourth power as the specific current is increased. Current is, of course, the most sensitive variable in the process. Similarly, it is not surprising that times above critical temperatures decrease in proportion with the square of the welding speed. Reduced welding speeds are often used as a method of improving mash seam weld quality.

Of interest, however, is the apparent relationship between the lap (y_0) and the time at welding temperatures. Equation 13 predicts that time above critical temperature will increase as the square of the lap. This observation explains a critical observation in mash seam welding mentioned above, that greater relative laps are strongly correlated to improvements in weld quality. The suggestion here is that the role of increased lap is not to increase forging during welding but rather to increase the heat content of the process, and increase the time above critical temperature.

Conclusions

In this program, the characteristics of welding have been analyzed in a theoretical way. To accomplish this analysis, mash seam welding has been considered in light of recent work on the basic mechanisms of solid-state welding. Central to these mechanisms of welding are the creation of surface strains and the addition of heat for thermally assisted processes. Analysis of surface strains was done through simple geometric relationships. Thermal analyses were done based on Rosenthal's 2-D heat-flow equations, coupled with a heat-generation term appropriate for resistance mash seam welding. Results provided a detailed picture of the operative mechanisms of welding for resistance mash seam welding, as well as an understanding of the major process factors. Specific conclusions include the following:

1) **Assessment of Surface Strains** — Surface strains can be easily calculated from a geometric analysis of the weld stackup. Final surface strains were simply a function of the relative joint thickness (Δ) and the relative lap of the sheets (ξ).
2) **Assessments of Thermal Cycles** — Thermal cycles can be estimated for resistance seam welding based on Rosenthal's 2-D heat-flow equation coupled with a heat-generation term appropriate for resistance mash seam welding. These simple models were extended to predict cooling rates and excursion times above critical temperatures.
3) **Weld Interface Strain Relationships for Mash Seam Welding** — Calculations of weld interface strains showed that the actual strain levels were largely a function of the setdown of the sheets, and insensitive to relative laps actually used for mash seam welding.
4) **Role of Surface Strains in the Formation of Mash Seam Welds** — Evaluated weld interface strains for real combinations of mash seam welding conditions suggested values typically less than 110%. This is only about one-quarter of the surface strain levels required for direct welding. Therefore, it appears that surface strains play a secondary role compared to thermal effects in the formation of mash seam-welded joints.
5) **Temperature Excursion Relationships for Mash Seam Welding** — Times above critical temperatures were found to be heavily dependent on the applied specific current, welding speed, and lap.
6) **Effects of Lap on Temperature Excursions** — Times above critical temperatures were found to increase as the square of the lap used. This suggests that a major influence of the lap is to extend the temperature excursion, rather than to increase the amount of forging in the workpiece.
7) **Operating Mechanisms of Joining for Mash Seam Welding** —These results suggest that thermally related effects are the dominant mechanisms of welding for this process, and that factors that increase time at temperature will inevitably improve weld quality.

References

1. Funk, E. J., and Bergeman, M. L. 1956. Electrical and metallurgical characteristics of mash seam welds. *Welding Journal* 35(6): 265-s to 274-s.

2. Adonyi, Y., Milian, J., and Roudabush, L. 1992. Welded steel sheet performance for tailored blanks. *Sheet Metal Welding Conference V.* Detroit, Mich.: AWS Detroit Section.

3. Gordon, H., and Corrodi, R. 1992. Blank welding — A new generation of blank welding machines. *Sheet Metal Welding Conference V*. Detroit, Mich.: AWS Detroit Section.

4. Geiermann, T. Published in IBEC conference proceedings.

5. Gould, J. E. 1995. Mechanisms of bonding for solid state welding processes. *ICAWT 95, Advances in Welding Processes.* Columbus, Ohio: Edison Welding Institute.

6. Tylecote, R. F. 1954. Investigations on pressure welding. *British Welding Journal* 1(3): 117–135.

7. Tylecote, R. F., Howd, D., and Furmidge, J. E. 1958. The influence of surface films on the pressure welding of metals. *British Welding Journal* 5(1): 21–38.

8. Mohamed, H. A., and Washburn, J. 1975. Mechanism of solid state pressure welding. *Welding Journal* 54(9): 302-s to 310-s.

9. Wright, P. K., Snow, D. A., and Tay, C. K. 1978. Interfacial conditions and bond strength in cold pressure welding by rolling. *Metals Technology* (1): 24–31.

10. Rosenthal, D. 1941. Mathematical theory of heat distribution during welding and cutting. *Welding Journal* 20(5): 220-s to 234-s.

11. Adams, C. M., Jr. 1958. Cooling rates and peak temperatures in fusion welding. *Welding Journal* 37(5): 210-s to 215-s.

12. Gould, J. E. 1987. An examination of nugget development during spot welding, using both analytical and experimental techniques. *Welding Journal* 66(1): 1-s to 10-s.